



MINNEAPOLIS • MAY 20-24, 2018

TRANSIENT RESPONSE OF A SQUEEZE FILM DAMPER TO IMPACT LOADS: EXPERIMENTS AND PREDICTIONS

CATEGORY Fluid Film Bearings

AUTHORS AND INSTITUTIONS

BONJIN KOO, Graduate Research Assistant

Texas A&M University, Mechanical Engineering Department, College Station, TX 77843-3123, USA

SUNG-HWA JEUNG, Compressor Design Engineer

Compressor Technology & Development, Ingersoll Rand, La Crosse, WI 54601, USA

LUIS SAN ANDRÉS, Mast-Childs Professor and Fellow STLE

Texas A&M University, Mechanical Engineering Department, College Station, TX 77843-3123, USA

INTRODUCTION

Squeeze film dampers (SFDs) provide damping to high-speed rotating machinery. In aircraft gas turbines, sudden maneuver loads, shock loads, or intermittent impact loads while landing compromise the reliability of the engine rotor-bearing system. A well-designed squeeze film damper (SFD) must aid in reducing rotor amplitude motions during these transient load events. Therefore, many researchers have poured efforts to clarify the dynamic characteristic of SFD subjected to transient loads.

Rotor-bearing system response to sudden loads is a firmly established field having tackled with fruition blade loss events [1-3], base seismic excitation [4,5]. The viscous damping available in a fluid film bearing or a SFD enables a system to survive seismic (base) load excitations, as shown in Refs. [4-5]. Roberts et al. [6,7] using time domain algorithms also extracted SFD parameters from measured transient response data and showed the damping and added mass coefficients are constants, nearly independent of amplitude of excitation. In these tests, the authors found mass coefficients exceeding a theoretical prediction, likely due to the influence of a central (oil feed) groove separating the film land into two parallel (not independent) sections. Recently, San Andrés and Jeung [8,9] recorded the transient response of an open ends SFD due to large amplitude impacts, single or as a series, sequential and intermittent to model a severe aircraft landing. As the magnitude of the impact load increases, the ensuing journal speed grows quickly (large acceleration) and the damper reacts with both a large fluid inertia force and a viscous dissipation force. Hence, the appearance of an added mass coefficient (M_{SFD}) produces a modest increase in the test system damping ratio since $\zeta \sim C/(M_{BC} + M_{SFD})$ where M_{BC} is the effective mass of the dry system. Also, Ref.[9] experimentally shows that the presence of fluid inertia tends to reduce the peak system dynamic response.

Using a test rig comprising a bearing cartridge (BC), an elastic support structure, and a SFD with film length $L=25.4$ mm, diameter $D=5L$, and clearance $c=254 \mu\text{m}$ ($D/c=500$), this extended abstract reports measurements of the test system transient response due to a sudden impulse load. The lubricant is an ISO VG 2 oil (viscosity $\mu=2.6$ cPoise and density $\rho=820 \text{ kg/m}^3$) that flows into the film land middle plane ($z=0$) through three feed holes ($\phi=2.5$ mm, 120° apart). On the axial ends of the film land, the journal has end grooves hosting piston rings (PRs) as end seals. The tests include SFD configurations with and without the PRs in place, i.e. sealed ends and open ends (to ambient). Note that a damper sealed with piston rings (PRs) provides a larger damping capability in a limited or confined space, short in axial length.

DESCRIPTION OF TEST RIG

Fig. 1 shows views of the SFD test rig with four elastic rods with lateral stiffness $K_s=10.0$ MN/m supporting a BC with $M_{BC}=15.2$ kg. The natural frequency of the dry system is $\omega_{n,dry}=\sqrt{K_s/M_{BC}}=129$ Hz and its damping ratio $\zeta_{dry}=0.03$. Hence, the structure damping $C_s=\zeta_{dry}(2\sqrt{K_s M_{BC}})=0.7$ kN-s/m. A hydraulic static loader pulls the BC to a static eccentric position (e_s) and two orthogonally placed shakers (X, Y) apply impact loads on the BC. Pairs of piezoelectric accelerometers and eddy current sensors record the BC acceleration and displacements relative to the rigid journal, and

two dynamic load cells measure the impact forces exerted on the BC.

FUNDAMENTALS OF SFD ANALYSIS MODEL

The dynamics of a point mass rotor supported on a SFD are

$$M_{BC}\ddot{\mathbf{r}} + C_s\dot{\mathbf{r}} + K_s\mathbf{r} = \mathbf{F}_{SFD} + \mathbf{F}_{ext} \quad (1)$$

where $\mathbf{r} = \{r_x, r_y\}^T$ is the journal displacement vector, and \mathbf{F}_{SFD} and \mathbf{F}_{ext} denote the vectors of squeeze film reaction force and externally applied load, respectively. C_s and K_s are the structure damping and stiffness coefficients, respectively. The motion starts from rest, hence the initial displacement and velocity are null.

The journal kinematics squeezes the film thickness (h) and produces a dynamic pressure field P governed by the extended Reynolds equation [10]

$$\nabla \cdot (h^3 \nabla P) = 12\mu \frac{\partial h}{\partial t} + \rho h^2 \frac{\partial^2 h}{\partial t^2}; \quad h = c - r_x \cos(\Theta) - r_y \sin(\Theta) \quad (2)$$

where Θ is an angular coordinate ($\Theta=0$ coincides with the X axis). At the oil feedholes ($z=0$), the supply pressure and orifice geometry define the supply flow rate [11]. The model regards the PRs as *local* ends seals, whose thru flow is proportional to the pressure drop ($P_{z=\pm L} - P_a$) and an empirical flow conductance coefficient [12].

Integration of the (numerically found) pressure field delivers the damper reaction force

$$\mathbf{F}_{SFD} = \begin{Bmatrix} F_x \\ F_y \end{Bmatrix} = - \int_{-L/2}^{L/2} \int_0^{2\pi} P_{(\theta,z,t)} \begin{Bmatrix} \cos \theta \\ \sin \theta \end{Bmatrix} R d\theta dz \quad (3)$$

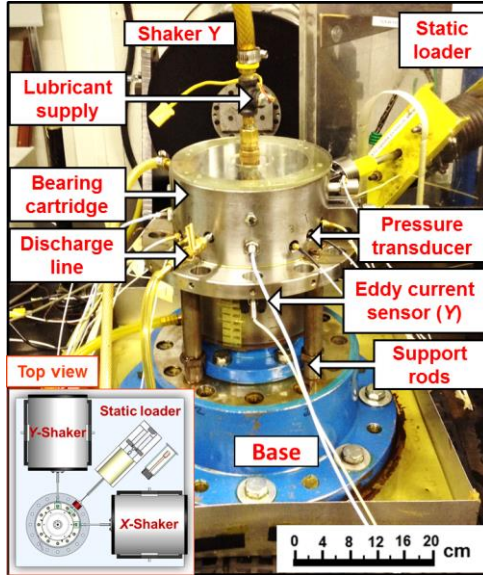


Fig. 1: Photograph and top view of SFD test rig [1].

TYPICAL RESULTS

For tests conducted with the open ends SFD and the sealed ends SFD, respectively, Fig. 2(a) depicts the delivered impact load (X direction) and the ensuing BC displacement (Z_x) vs. time. In the graphs, top to bottom, the peak impact load $F_{MAX}/(LD)$ increases from 1.6 bar to 6.2 bar.

The motion (Z_x) about the bearing center ($e_s=0$) is oscillatory with an envelope decaying exponentially, typical of a viscous damped system. Expectedly, the transient response for the system with a PR sealed SFD decays faster and shows smaller peak BC displacement (Z_{X-MAX}) than that with an open ends SFD. That is, the BC displacement (Z_{X-MAX}/c) for the open ends SFD ranges from $\sim 0.1 - 0.4$; while for the sealed ends SFD, Z_{X-MAX}/c ranges from $\sim 0.05 - 0.2$.

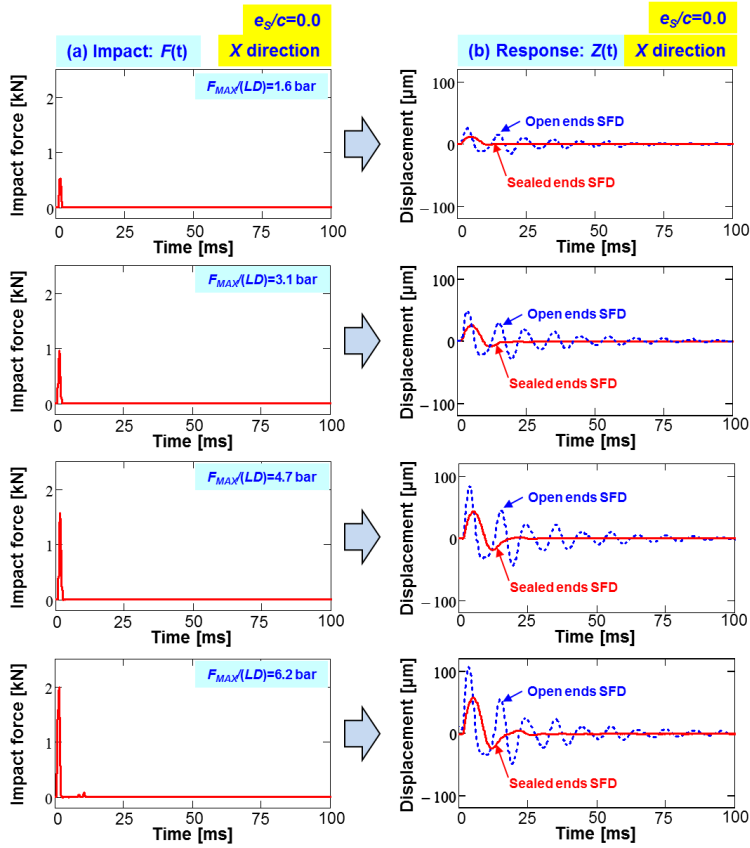
For the open ends SFD and sealed ends SFD, the system natural frequency $\omega_n = \sqrt{\frac{K_s}{M_{BC} + M_{SFD}}} = \frac{2\pi}{\tau_n} \sim 116$ Hz and 83

Hz, respectively, lower than that for the dry system $\omega_{n,dry}=129$ Hz. Note a typical impact load lasts ~ 1.3 ms, a small fraction of the natural period of motion, $\tau_{n,dry}=7.7$ ms.

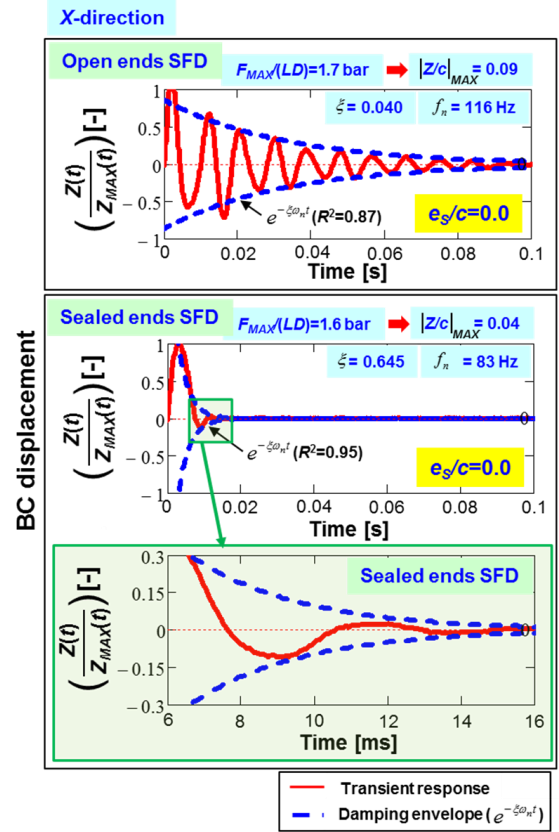
The damping ratio $\zeta = C/2\sqrt{K_s M}$ for the test system can be easily derived from the logarithm decrement (δ) which relates the motion peak amplitude (\bar{Z}) decay between successive peaks of displacement. In brief, for N spaced periods of motion [13],

$$\delta = \frac{1}{N} \ln \left(\frac{\bar{Z}_k}{\bar{Z}_{k+N}} \right) = \frac{2\pi\zeta}{\sqrt{1-\zeta^2}} = \zeta \omega_n \tau_d \quad (4)$$

For an impact with peak amplitude $F_{MAX}/(LD)=1.6$ bar, Fig. 2(b) depicts the system transient response (Z_x) and the damping envelope curve ($e^{-\zeta\omega_n t}$) vs. time. The top graph represents the response of the open ends SFD whereas the bottom graph corresponds to the response of the PR-SFD. A curve fit of six displacement peaks for the open ends SFD and three peaks for the PR-SFD produces $\delta \rightarrow \zeta$. For easy comparison, the displacement (Z_x) is normalized with respect to the peak amplitude, (Z/Z_{MAX}). Note the majority of the envelope fits ($e^{-\zeta\omega_n t}$) shows a high correlation factor ($R^2 > 0.9$) with the test data.



(a) Impact load and dynamic displacement



(b) Dimensionless BC displacement

Fig. 2 (a) Transient response Z_x vs. time for open ends SFD (top) and sealed ends SFD (bottom) due to a single impact load, $F_{MAX}(LD)=1.6$ bar - 6.2 bar; (b) Z/Z_{MAX-X} and envelope ($e^{-\zeta\omega_n t}$) vs. time for impact with $F_{MAX}(LD)=1.6$ bar.

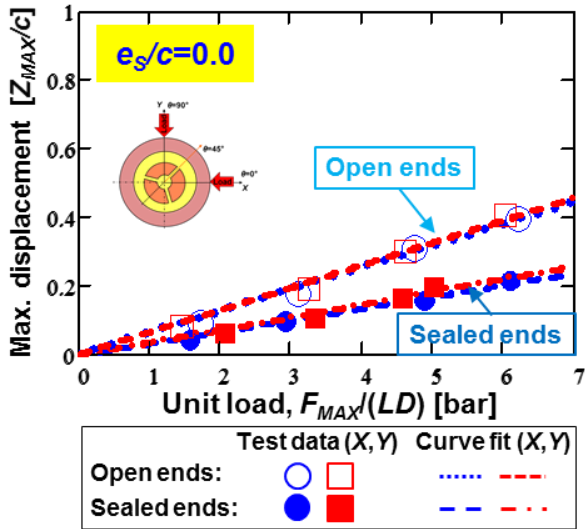


Fig. 3. Maximum displacement Z_{MAX}/c vs. peak amplitude of impact $F_{MAX}(LD)$ for motions initiating from bearing center. Open-SFD and PR-SFD. Clearance $c=0.254$ mm.

Fig. 3 depicts the maximum BC displacement Z_X/c versus the peak amplitude of the impact load ($F_{MAX}(LD)$) applied along the X or Y directions for motions initiating from the bearing center $e_s/c=0.0$. The dashed lines show a linear regression fit, and which evidences a proportional relationship between the maximum BC displacement and the peak amplitude of the impact load.

Fig. 4 shows predictions and measurements of the test system displacement Z/Z_{MAX-X} vs. time. The graphs also include the damping envelope ($e^{-\zeta\omega_n t}$) and display the system natural frequency for the test data and analysis. For the open ends SFD (top graph), the predicted and experimentally estimated damping ratios ($\zeta \sim 4\%$) match whereas the natural frequency is $\sim 8\%$ overly predicted, which means the predicted fluid added mass (0.63 kg) is small compare to the estimated from the test (3.6 kg). The natural frequency and damping ratio is identified from the first three cycles. The discrepancy in the natural frequencies shows an increasing phase difference between predictions and measurements.

For the PR sealed SFD (bottom graph), the predicted natural frequency agrees with the measured one; however the damping ratio ($\zeta \sim 0.43$) is about $\sim 66\%$ of the one estimated from the measured data ($\zeta \sim 0.65$). The predicted and estimated damping coefficients ($C_{sealed\ SFD}$) are ~ 16 kN-s/m and ~ 25 kN-sm, respectively, showing a discrepancy of $\sim 36\%$.

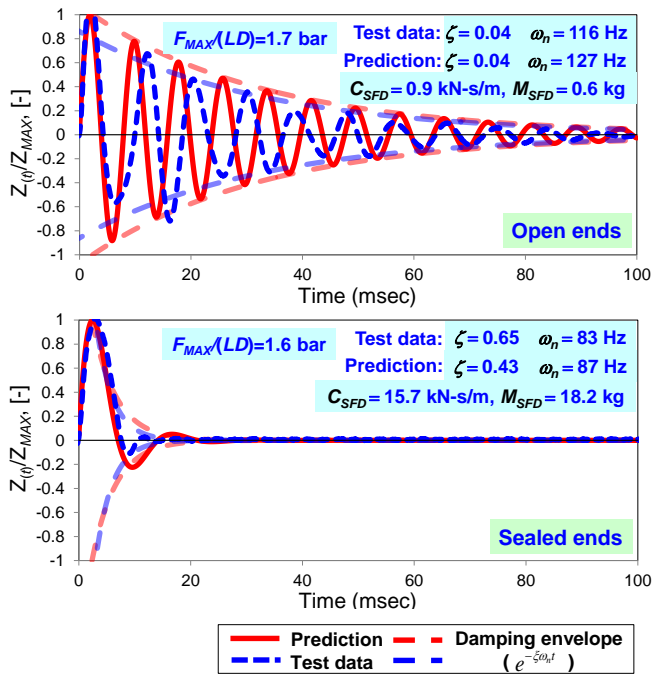


Fig. 4 Measured and predicted BC displacement (Z/Z_{MAX-x}) and damping envelope ($e^{-\zeta\omega_n t}$) vs. time due to a single impact load, $F_{MAX}(LD)=1.6$ bar. (Top) open ends SFD, (bottom) PR-SFD.

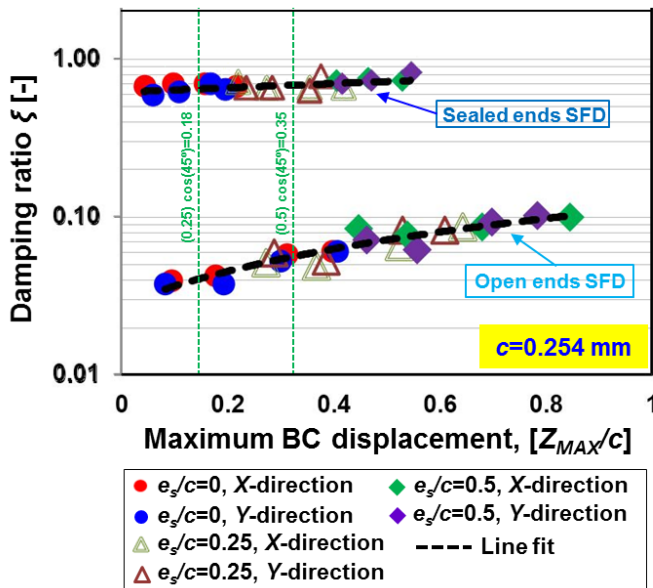


Fig. 5 System damping ratio (ξ) and logarithmic decrement (δ) versus peak BC (Z_{MAX}/c) displacement. Data for one impact load and motions departing from various static eccentricity. Open ends SFD and sealed ends SFD with $c=0.254$ mm.

REFERENCES

- [1] San Andrés, L., Den, S., and Jeung, S.-H., 2016, "Transient Response of a Short-Length ($L/D=0.2$) Open Ends Elastically Supported Squeeze Film Damper: Centered and Largely Off-Centered Whirl Motions," *ASME J. Gas Turb. Pwr.*, **138**(12), pp. 122503.

The discrepancy in the damping coefficient (C_{SFD}), under-predicted, relies on a likely improper end seal flow resistance used in the analysis. A small end flow resistance allows for more leakage through the seal and generates lesser damping.

Fig. 5 (note the logarithmic scale) shows the estimated test system damping ratio (ζ) obtained for the sealed ends SFD and the open ends SFD vs. the maximum displacement (Z_{MAX}/c). For the open ends and sealed ends SFDs, the lubricant supply pressures (P_{in}) are 0.35 bar(g) and 0.69 bar(g), respectively. The test data corresponds to a single impact and motions departing from static eccentricity $e_s=0$, $\frac{1}{4}c$, and $\frac{1}{2}c$. Both sealed ends and open ends dampers show an increase in damping ratio (ζ) with an increase in static eccentricity (e_s).

The sealed ends SFD provides ten to sixteen times more damping ratio (ζ) than the open ends configuration. More interestingly, the damping ratio for the open ends SFD increases quickly with the peak displacement. This may indicate that the fluid inertia decreases faster than the viscous damping when air ingests thru the axial ends.

CONCLUSION

The abstract describes the dynamic response of a test SFD (open ends and end sealed) to impact load tests. As expected from a linear system, during the transient response, the peak displacement (Z_{MAX}) is proportional to the amplitude of the impact (F_{MAX}).

The sealed ends damper shows ten to sixteen times more damping ratio (ζ) than that for the open ends SFD. That is, $\zeta_{sealed\ SFD} \sim 0.6-0.8 > \zeta_{open\ SFD} \sim 0.04$ to 0.1. The natural frequency for the sealed SFD system is much lower than that for the open SFD hence denoting a large added mass effect.

The paper also briefs on a physical model to predict the response of the test system and including the instantaneous SFD reaction force during the sudden event. The predictions agree well with the measurements as per peak amplitude of motion and the time at which it happens. However, the predictions show a discrepancy in the natural frequency (due to a difference in M_{SFD}) compared to the measurements for the open ends SFD in particular. The discrepancy in the natural frequency demonstrates the importance of film fluid inertia to accurately characterize the test SFD forced response.

ACKNOWLEDGMENTS

The authors gratefully acknowledge the continued financial support from the TAMU Turbomachinery Research Consortium. The authors also thank Pratt & Whitney Engines (UTC) for their continuous support and interest. Special thanks to undergraduate student Scott Tran for performing a number of the experiments.

- [2] Stallone, M. J., Gallardo, V., Storace, A. F., Bach, L. J., and Black, G., 1983, "Blade Loss for Transient Dynamic Analysis of Turbomachinery," *AIAA J.* **21**(8), pp. 1134-1138.
- [3] Zhang, S. P., Yan, L. T., and Li, Q. H., 1991, "Development of Porous Squeeze Film Damper Bearings for Improving the Blade Loss Dynamics of Rotor-Support Systems," *ASME J. Vib., Acoust.*, **114**, pp. 347–353.
- [4] Hori, Y, Kato, T., 1990, "Earthquake-Induced Instability of a Rotor Supported by Oil Film Bearings," *ASME J. Vibr. Acoust.*, **112**, pp.160–165.
- [5] Lee, A., Kim, B., and Kim, Y., 2006, "A Finite Element Transient Response Analysis Method of a Rotor-Bearing System to Base Shock Excitations Using the State-Space Newmark Scheme and Comparisons With Experiments," *J. Sound Vib.*, **297**(3–5), pp. 595–615.
- [6] Roberts, J. B., Holmes, R., and Mason, P. J., 1986 "Estimation of Squeeze-Film Damping and Inertial Coefficients from Experimental Free-Decay Data," *ImechE Proc., Engineering Sciences Division*, **200**(2C), pp. 123-133.
- [7] Ramli, M. D., Roberts, J. B., and Ellis, J., 1987, "Determination of Squeeze Film Dynamic Coefficients from Experimental Transient Data," *ASME J. Tribol.*, **109**, pp. 155–163.
- [8] San Andrés, L., and Jeung, S.-H., 2015, "Response of a Squeeze Film Damper to Large Amplitude Impact Loads," 2015 STLE Annual Meeting & Exhibition, May 18-21, Dallas, TX, USA.
- [9] San Andrés, L., and Jeung, S.-H., 2016, "Response of a Squeeze Film Damper-Elastic Structure System to Multiple and Consecutive Impact Loads," *ASME J. Eng. Gas Turb. Pwr.*, **138**(12), p.122504.
- [10] Delgado, A., and San Andrés, L., 2010, "A Model for Improved Prediction of Force Coefficients in Grooved Squeeze Film Dampers and Oil Seal Rings," *ASME J. Tribol.*, **132**(3), pp. 032202.
- [11] San Andrés, L., Koo, B., Jeung, S.-H., 2018, "Experimental Force Coefficients for Two Sealed Ends Squeeze Film Dampers (Piston Rings and O-rings): An Assessment of their Similarities and Differences," *Proc. of ASME Turbo Expo 2018: Turbine Technical Conference and Exposition*, GT2018-76224, June 11-15, Oslo, Norway.
- [12] Marmol, R. A., and Vance, J. M., 1978, "Squeeze Film Damper Characteristics for Gas Turbine Engine," *ASME J. Tribol.*, **100**, pp. 139-146.
- [13] Ginsber, J. H., 2001, *Mechanical and Structural Vibration-Theory and Application*, John Wiley & Sons, New York, pp. 79-85.

KEYWORDS

Hydrodynamics: Squeeze-Film Dampers, Engines: Gas/Jet Turbines.